Pulse propagation in a simple probabilistic transport model

B. Ph. van Milligen 1), B. A. Carreras 2), V.E. Lynch 2), R. Sánchez 2)

1) Asociación EURATOM-CIEMAT para Fusión, Avda. Complutense 22, 28040 Madrid, Spain
2) Fusion Energy Division, Oak Ridge National Laboratory, P.O. Box 2001, Oak Ridge TN 37831-2001, USA

e-mail contact of main author: boudewijn.vanmilligen@ciemat.es

Abstract. The response to perturbations of a simplified transport model is studied. The model is used as a paradigmatic example of transport controlled by a critical gradient. Long-time system behaviour is diffusive when most of the system is sub-critical. However, when the critical mechanism becomes significant, it is observed to dominate the system behaviour at both short and long time scales. While the pulse amplitude decays in an approximately diffusive manner at long times for weakly critical situations, the pulse shape is not self-similar and cannot be modelled using a single transport exponent.

1. Introduction

In recent work [1-6] we have designed a simplified model for transport in fusion plasmas, based on the Continuous Time Random Walk (CTRW) formalism [7,8], which incorporates a critical gradient mechanism. It was shown to reproduce much of the unusual phenomenology observed in actual fusion experiments (power degradation, profile stiffness, rapid propagation of perturbations, uphill transport), which is the prime reason for continued study of this particular model. Moreover, the model provides a test-bed for advancing understanding of the critical gradient mechanism, central to many models for transport in fusion plasmas in view of ample supportive experimental evidence [9-13]. This feature is explored in the present work, in which the response of the model to localized perturbations is studied.

2. The model

The model is described in considerable detail elsewhere and the reader is referred to the cited references for more information. Here we note only that the simplified model is Markovian in nature and that the time evolution of the single field $n(x,t)$, which may be interpreted as a (particle) density, can be described, in one dimension, by a Generalized Master Equation:

$$\frac{\partial n}{\partial t} = \frac{1}{\tau_D}\left[\int_0^1 dx'\, p(x-x',x',t)n(x',t)\right] - \frac{n(x,t)}{\tau_D} + S(x) \qquad (1)$$

The domain of the system is $0 \le x \le 1$. $\tau_D = 1$ is a "waiting time" and $S(x)$ a source (taken constant in time), needed to compensate edge losses associated with the absorbing boundary conditions imposed at $x = 0, 1$. The function p is a "particle step distribution". Standard diffusion is recovered with a Gaussian step distribution, $p(x–x',x',t) = G(x–x',\sigma) = exp[–(x–x')^2/4\sigma^2]/2\sigma\sqrt{\pi}$ in the limit of small σk (k being the wave-vector): i.e. $\partial n/\partial t = \partial^2/\partial x^2[\sigma^2 n/\tau_D] + S$. Thus, the model is closely related to standard transport models in common use, while allowing a critical mechanism to be incorporated in a mathematically sound way (cf. the cited references).

For the present study, the most important element of the model is the step distribution p, which is chosen as follows to produce the required critical gradient mechanism:

$|\nabla n| < [\nabla n]_{crit}$: sub-critical or "normal" transport; $p = p_0$

$|\nabla n| \ge [\nabla n]_{crit}$: super-critical or "anomalous" transport; $p = p_1$

Here, p_0 and p_1 are fixed and symmetric stable probability distributions (of the Lévy type, of which the Gaussian is a special case). Transport at any given location x will therefore be normal

or anomalous as a function of the local value of the density gradient. This introduces a mechanism for self-regulation into the model.

3. Numerical studies

The numerical calculations are performed on a grid with $N = 2000$ grid points ($0 \le x \le 1$), using standard integration techniques for stiff differential equations to advance Eq. (1) in time [14]. The source $S(x) = S_0$ is taken constant.

Throughout this paper, we set $p_0 = G(x–x',\sigma_0)$ with $\sigma_0 = 0.002$, while $p_1 = G(x–x',\sigma_1)$ with $\sigma_1 = 0.008$ for the cases labelled "Gauss-Gauss" (both transport channels are Gaussian), or $p_1 = C(x–x',\sigma_1) = \sigma_1/\pi(\sigma_1^2+(x–x')^2)$ with $\sigma_1 = 0.004$ for the cases labelled "Gauss-Cauchy" (sub-critical transport Gaussian, super-critical transport Cauchy). The critical gradient is chosen $[\nabla n]_{crit} = 2000$.

3.1 Gauss-Gauss; negative perturbation

The source rate was varied in the range $0.01 \le S_0 \le 10$. In this range, the system transits from a sub-critical to a super-critical situation, analogous to what has been reported in Ref. [1]. Steady state profiles are shown in Fig. 1 for the Gauss-Gauss case. At $S_0 = 0.01$, the profile is parabolic and the system is sub-critical (purely diffusive). In the range $0.05 \le S_0 \le 1$, ever larger parts of the profile are critical, as is evident from the sections with constant gradient in the profiles. At $S_0 = 10$, the profile is parabolic again, and thus dominantly super-critical.

To probe the reaction of the system to negative perturbations, we multiply the steady state profile $n(x,0)$ by the factor

$$f(x) = (1–\exp[–(x–x_0)^2/2w^2])(1–\exp[–(x–1+x_0)^2/2w^2]) \quad (2)$$

with $w = 0.005$ and $x_0 = 0.125$. This way, the profile is perturbed by a double narrow negative density pulse centred at x_0 and $1–x_0$. Then, the evolution of this perturbation is followed in time. Figs. 2 and 3 show the initial evolution of the perturbation (shown is the profile $\tilde{n}(x,t) = n(x,t)-n(x,0)$, where $t=0$ corresponds to a time immediately previous to the density perturbation at $t=0.11$). We note that the negative density perturbation produces a small-amplitude *positive* perturbation that propagates outward from the locations of the perturbation in a nearly ballistic fashion (at constant speed). The formation of these positive perturbations is related to flux accumulation between zones with super-critical (fast) and sub-critical (slow) transport. Between times $t = 3$ and 4, the ballistic propagation of the front halts and further evolution is mostly diffusive in nature. We conclude that the model shows two modes of propagation: a ballistic

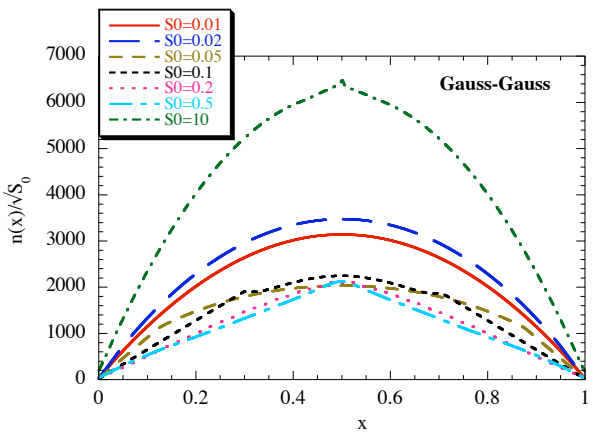

Fig. 1 – Steady-state profiles of n(x), normalized by $\sqrt{S_0}$ for display purposes, for various values of S_0.

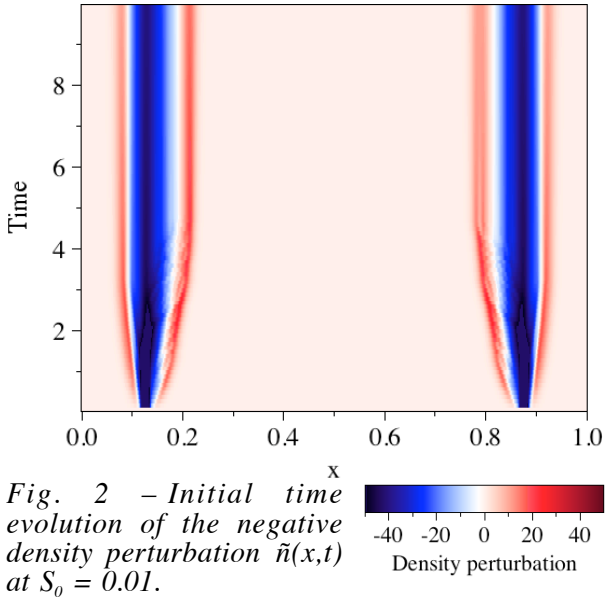

Fig. 2 – Initial time evolution of the negative density perturbation $\tilde{n}(x,t)$ at $S_0 = 0.01$.

propagation of the perturbation front (cf. Ref. [15]), associated with the criticality mechanism (i.e. the profile stiffness), and normal diffusive behaviour that takes over as soon as the gradients drop to around or below the critical value. Evidently, in the small amplitude limit of the perturbation, the model would respond purely diffusively in this case (without pulse fronts).

This observation leads us to expect the long-time behaviour of the model to be diffusive in this (sub-critical) case. Fig. 4 shows the long-time behaviour of the perturbation. Indeed, the negative perturbation spreads out and becomes shallower in a diffusive manner, and no drifts (associated with convection) in the position of the negative perturbations are apparent.

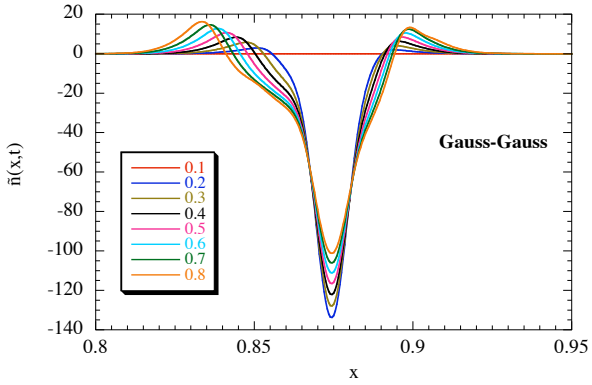

Fig. 3 – The first few profiles of ñ(x,t) shown in Fig. 2, around the point 1–x_0, at the indicated times t, showing the gradual formation of the positive perturbation fronts.

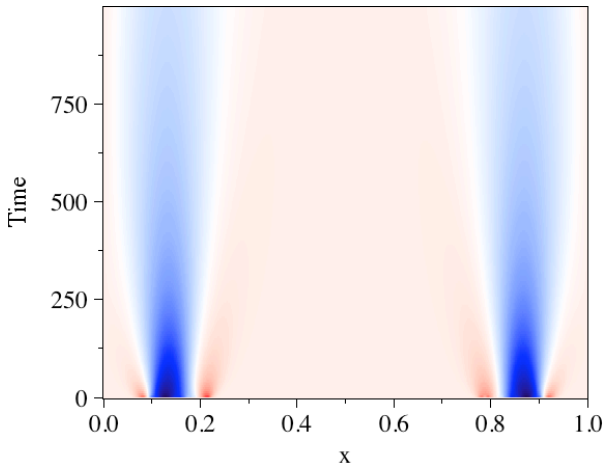

Fig. 4 – Long- time behaviour of the density perturbation ñ(x,t) shown in Fig. 2. (Same colour scale as Fig. 2.)

To quantify the long-time evolution, we note that the density perturbation at the position of the initial perturbation x_0 is expected to behave like

$$-\tilde{n}(x_0,t) \cong ct^{-1/\alpha} \tag{3}$$

where the exponent α is associated to the transport mechanism, α being 2 for a Gaussian (diffusive) process. Fig. 5 shows this quantity, along with a fit to Eq. (3) for the long-time behaviour. The fit is consistent with $\alpha = 2$. Also note the initial transient for small t ($t \leq 4$), associated with the observation reported in Figs. 2-3.

A second diagnostic of the long-time properties of the perturbations is to determine, for a given position x, the time t_M at which the negative perturbation is maximum (excluding times in the initial transient range, $t \leq 10$). This time is expected to scale like

$$t_M = c_M\, |x-x_0|^{\alpha} \tag{4}$$

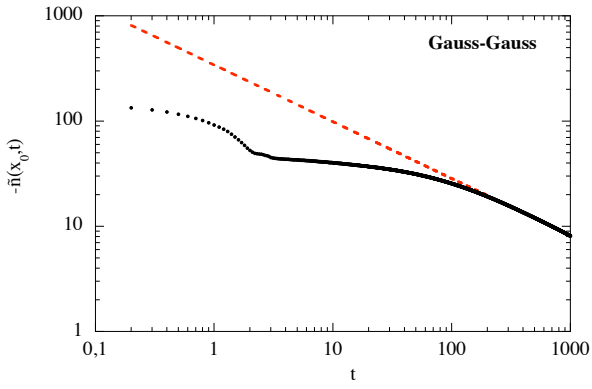

Fig. 5 – Time evolution of $-\tilde{n}(x_0,t)$ and fit at long times (dashed line: $\tilde{n} \propto t^{-0.540}$), at $S_0 = 0.01$.

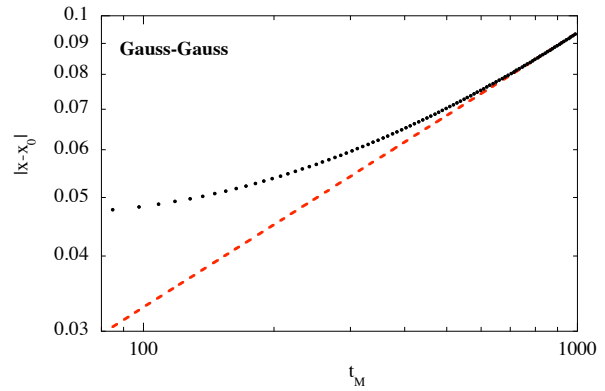

Fig. 6 – Time t_M of the maximum negative perturbation vs. distance from the initial perturbation $|x–x_0|$, and fit (dashed line: $|x–x_0| \propto t_M^{0.455}$), at $S_0 = 0.01$.

This analysis is performed in Fig. 6 for the inward travelling part of the perturbation (the outward part being distorted by the presence of the system boundary). We obtain $\alpha \approx 2.2$, reasonably close to expectation, considering that full convergence to the asymptote would require a longer experiment (and much CPU time).

A repetition of the experiment at increasing values of S_0 is shown in Fig. 7. The cases $S_0 = 0.01$, 0.02 and 0.05 are qualitatively very similar, although the positive perturbation front is ever more important, related to the increased stiffness of the profile (quantifiable using e.g. the criterion of Ref. [16]). A qualitative change occurs at $S_0 = 0.1$, the first case at which the perturbed location is critical. Nearly instantaneous communication of the perturbation across the critical region is observed, and the positive front is generated *inside* the innermost critical position. At $S_0 = 0.2$, most of the profile is critical and the effect of the perturbation is communicated nearly instantaneously over the whole system. Subsequently, very complex behaviour is observed. At $S_0 = 0.5$, this instantaneous system-wide communication is maintained, but dynamics are simplified due to extreme stiffness in the region between the centre and the perturbation. The observed behaviour is certainly not describable by any simple diffusive model.

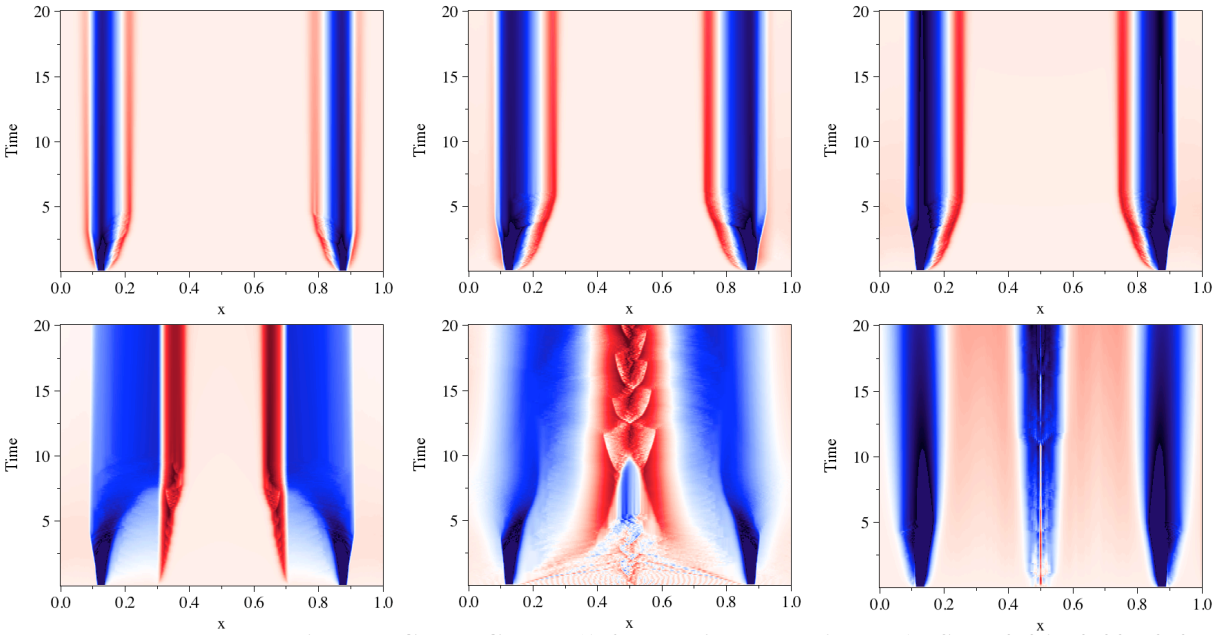

Fig. 7 – Negative perturbation, Gauss-Gauss; (left to right, top to bottom): $S_0 = 0.01$, 0.02, 0.05; 0.1, 0.2, 0.5. (Same colour scale as Fig. 2.)

Due to the fact that the centre of the negative pulse now exhibits a drift in time, the diagnostic of Eq. (3) must be adapted: instead of determining the temporal evolution of $\tilde{n}$ at x_0, we determine it at the position of the minimum of $\tilde{n}$ for every time t. The resulting curves are shown in Fig. 8.

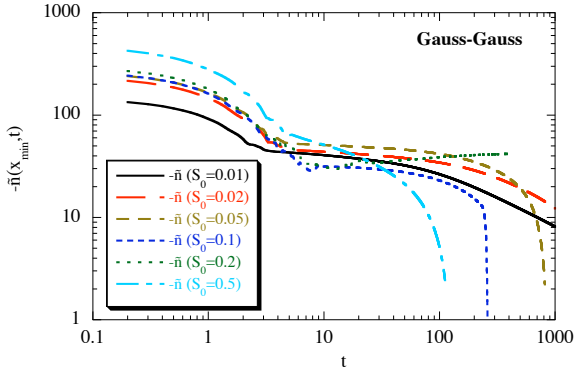

Fig. 8 – Evolution in time of –min(ñ) in the range ($0.65 \le x \le 1$).

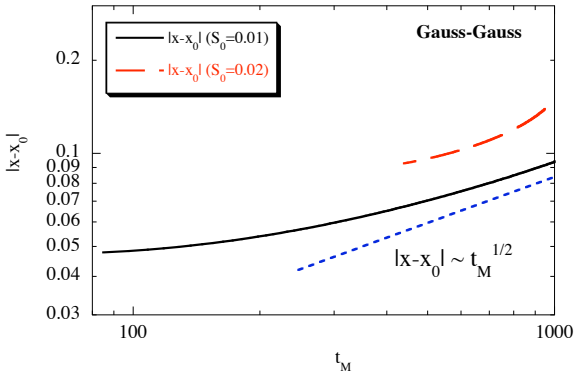

Fig. 9 – Time t_M of the maximum negative perturbation vs. distance from the initial perturbation $|x–x_0|$.

It shows that at low values of S_0, the system behaves diffusively (the amplitude decays like $t^{-1/2}$) for large t, while at $S_0 \geq 0.05$, the decay is much more rapid due to stiffness; the restoration of the gradient to its critical value is at least exponentially fast. Fig. 9 shows the evolution of the position of the maximum negative perturbation. This diagnostic does not work well when the propagation is not simple (i.e. when stiffness effects are important), so results are only given for the low S_0 cases.

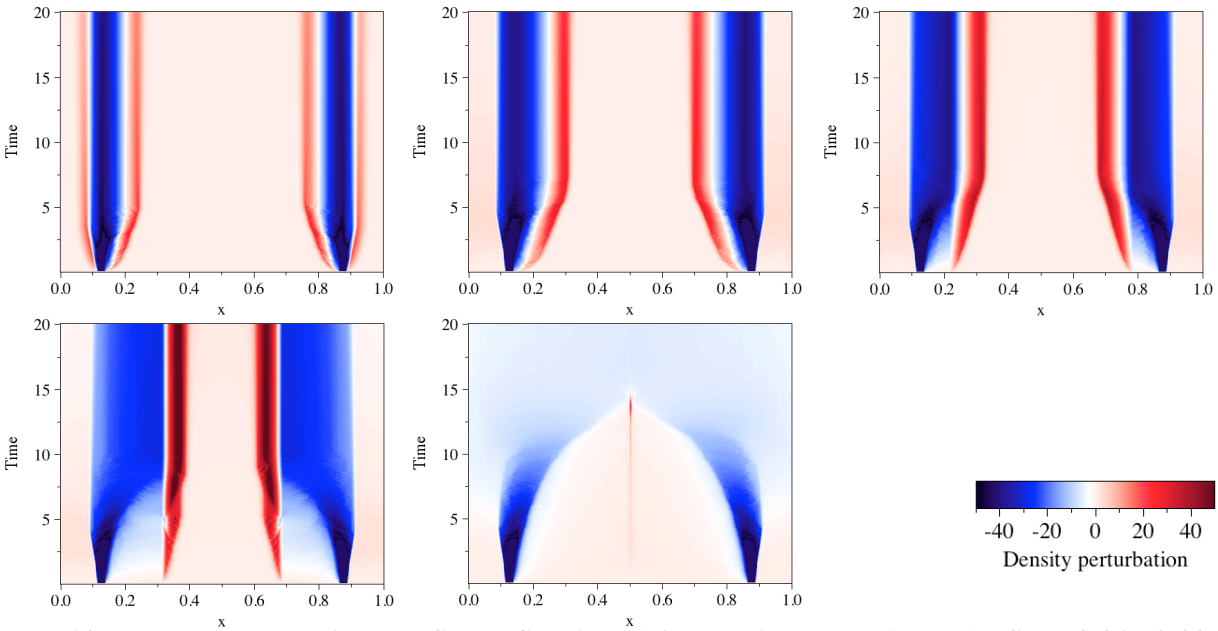

Fig. 10 – Negative perturbation, Gauss-Cauchy; (left to right, top to bottom): S_0 = 0.01, 0.02, 0.05; 0.1, 0.2.

3.2 Gauss-Cauchy; negative perturbation

The series of experiments is repeated for the Gauss-Cauchy case. Super-critical transport is now qualitatively different (i.e. long-range). Fig. 10 shows the initial time evolution of the perturbation. The figure is quite similar to Fig. 7, except for two points: the separation of the positive pulse generating point from x_0 occurs already for S_0 = 0.05 (in accordance with the greater extent of the critical region), while the system is already critical over the full radius in the case S_0 = 0.2. Both these effects can be attributed to increased system stiffness, due to the increased transport capacity of the super-critical transport channel.

The analysis of transport exponents is shown in Figs. 11 and 12. In Fig. 11, only the lowest fuelling level (S_0 = 0.01) shows asymptotic diffusive behaviour. Higher fuelling levels show a decay of the perturbation that is at least exponentially fast. The analysis shown in Fig. 12 does not allow the determination of a useful transport exponent.

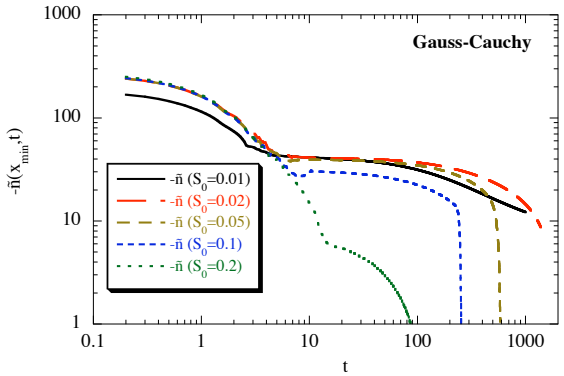

Fig. 11 – Evolution in time of –min(ñ) in the range (0.65 ≤ x ≤ 1).

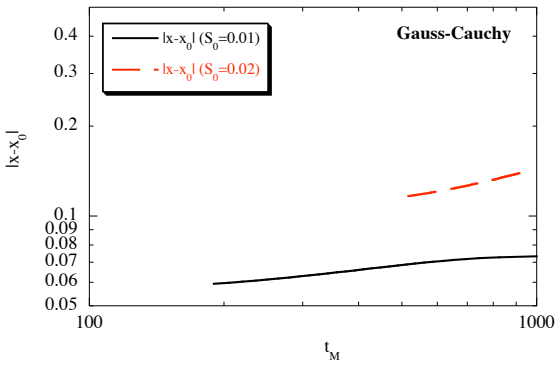

Fig. 12 – Time t_M of the maximum negative perturbation vs. distance from the initial perturbation $|x–x_0|$.

3.3 Gauss-Gauss; positive perturbation

To probe the reaction of the system to a central positive perturbation, we multiply the steady state profile $n(x,0)$ by the factor

$$f(x) = (1+\varepsilon \exp[-(x-x_0)^2/2w^2]) \quad (5)$$

with $\varepsilon = 0.25$, and $x_0 = 0.5$. This produces a single positive perturbation at the system centre with width w. Some examples of the initial evolution are shown in Fig. 13, for a sub-critical and a critical case, and various values of w.

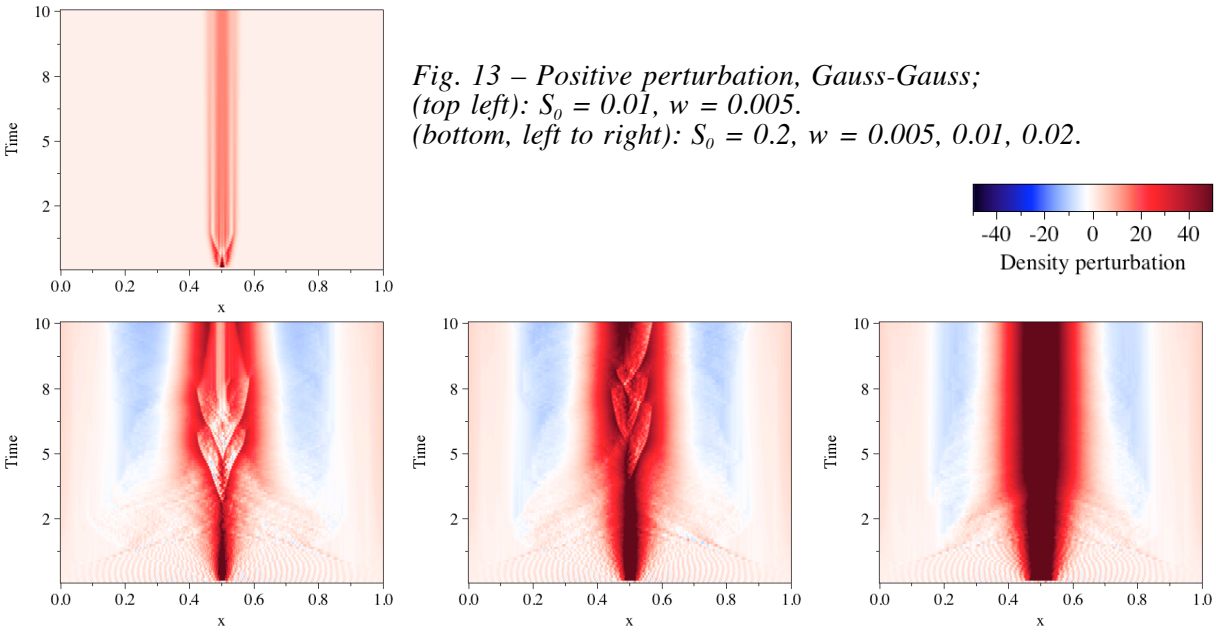

Fig. 13 – Positive perturbation, Gauss-Gauss; (top left): $S_0 = 0.01$, $w = 0.005$. (bottom, left to right): $S_0 = 0.2$, $w = 0.005, 0.01, 0.02$.

The analysis of transport exponents is shown in Fig. 14. For sufficiently low values of S_0 (S_0 =0.01), the behaviour is diffusive after an initial transient. However, for high values of S_0 (S_0 =0.2), relaxation does not occur on the timescales studied, and therefore no transport exponent could be determined.

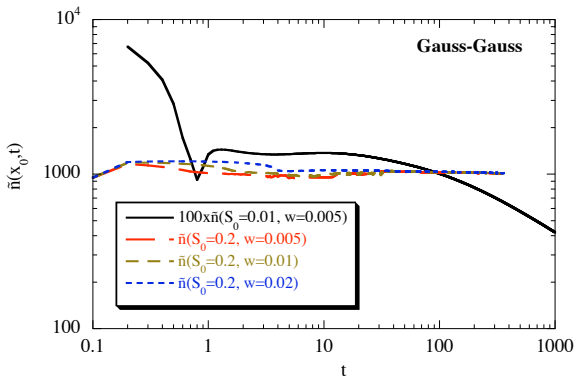

Fig. 14 – Evolution in time of $\tilde{n}(x_0,t)$.

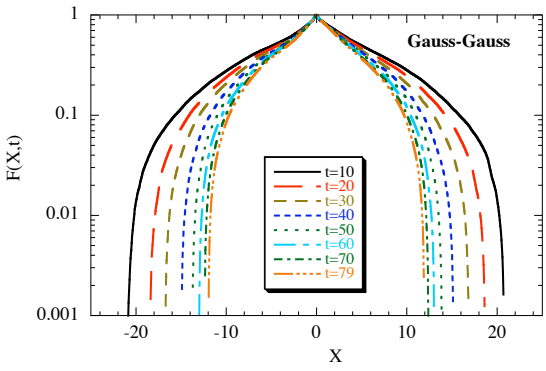

Fig. 15 – Renormalised pulse shape at various times. $S_0 = 0.2$, $w = 0.005$.

In view of the observed complexity of the transport behaviour, we pose the question whether the profile evolution is at all self-similar for times greater than the initial transient time. If that were the case, then the evolution could still be described by a single transport exponent, in spite of its complexity. To answer this question, we plot the renormalized perturbation:

$$F(X,t) = \tilde{n}(x,t)/\tilde{n}(x_0,t), \text{ with } X = \tilde{n}(x_0,t)(x-x_0) \quad (6)$$

This quantity is shown for various times in Fig. 15 for the case $S_0 = 0.2$, $w = 0.005$. The centre of the pulse is nearly self-similar, but at increasing times the wings are narrower than one would expect from the central decay. The absence of self-similarity means that the evolution cannot be described by any single transport exponent. It should be noted that the central decay rate alone (Fig. 14) might suggests a simple scaling behaviour for long times, so that one might be tempted to model the system using (fractional) differential equations, but the self-similarity test shows that this is an unsatisfactory description of the overall behaviour. Caution is therefore needed when analysing measurements made on critical systems, since the central decay rate is what typically might be obtained from a low-resolution measurement of pulse propagation.

4. Conclusions

To understand transport in systems controlled by a critical gradient, believed to be relevant for transport in fusion devices, the response to perturbations was studied in a simplified numerical model. The comparison between the cases Gauss-Gauss and Gauss-Cauchy reveals that the nature of the super-critical transport channel (Gauss or Cauchy) has little influence on the propagation of the perturbations, which is very similar in both sets of cases. Thus, the critical mechanism dominates the behaviour of the system.

The long-time behaviour of the system, as measured using two related techniques, is mostly diffusive at low fuelling rates, regardless of the case type; while no single transport exponent can describe the behaviour at high fuelling rates. However, on short timescales, the system behaviour is extremely non-diffusive in all cases, showing rapid ("ballistic" or even "instantaneous") propagation and perturbation sign reversal. A self-similarity test of the pulse shape confirms that the long-range behaviour is non-diffusive at high fuelling rates and cannot even be characterised by a single transport exponent, eliminating any hope of modelling these systems using a single effective (fractional) diffusive operator. The origin of this behaviour must be sought in the stiffness properties of the system.

The observations presented here, reported for simulations performed using a simplified transport model, are believed to be relevant to the understanding of transport (and of the propagation of perturbations) in fusion devices, where critical mechanisms are thought to be operative and profile stiffness is often observed.

Acknowledgements

This research was sponsored in part by DGI (Dirección General de Investigación) of Spain under Project No. FTN2003-08337-C04-02 and ENE2004-04319. Part of this research sponsored by the Laboratory Research and Development Program of Oak Ridge National Laboratory, managed by UT-Battelle, LLC, for the U.S. Department of Energy under contract number DE-AC05-00OR22725.

References

[1] VAN MILLIGEN, B.Ph., SÁNCHEZ, R., and CARRERAS, B.A., "Probabilistic finite-size transport models for fusion: anomalous transport and scaling laws", Phys. Plasmas **11** (2004) 2272.

[2] VAN MILLIGEN, B.Ph., CARRERAS, B.A., and SÁNCHEZ, R., "Uphill transport and the probabilistic transport model", Phys. Plasmas **11** (2004) 3787.

[3] VAN MILLIGEN, B.Ph., CARRERAS, B.A., and SÁNCHEZ, R., "The foundations of diffusion revisited", Plasma Phys. Control. Fusion **47** (2005) B743.

[4] SÁNCHEZ, R, CARRERAS, B.A., and VAN MILLIGEN, B.Ph., "Fluid limit of nonintegrable continuous-time random walks in terms of fractional differential equations", Phys. Rev. E **71** (2005) 011111.

[5] SÁNCHEZ, R, VAN MILLIGEN, B.Ph., and CARRERAS, B.A., "Probabilistic transport models for plasma transport in the presence of critical thresholds: Beyond the diffusive paradigm", Phys. Plasmas **12** (2005) 056105.

[6] CARRERAS, B.A., LYNCH, V.E., VAN MILLIGEN, B.Ph., and SÁNCHEZ, R., "On the use of critical gradient models in fusion plasma transport studies", Phys. Plasmas **13** (2006) 062301.

[7] MONTROLL, E.W., and WEISS, G.H., "Random walks on lattices. II", J. Math. Phys. **6** (1965) 167.

[8] BALESCU, R., "Anomalous transport in turbulent plasmas and continuous time random walks", Phys. Rev. E **51** (1995) 4807.

[9] BAKER, D.R., GREENFIELD, C.M., BURRELL, K.H., *et al.*, "Thermal diffusivities in DIII-D show evidence of critical gradients", Phys. Plasmas **8** (2001) 4128.

[10] RYTER, F., TARDINI, G., DE LUCA, F., *et al.*, "Electron heat transport in ASDEX Upgrade: experiment and modelling", Nucl. Fusion **43** (2003) 1396.

[11] RYTER, F., ANGIONI, C., PEETERS, A.G., *et al.*, "Experimental study of trapped-electron-mode properties in tokamaks: threshold and stabilization by collisions", Phys. Rev. Lett. **95** (2005) 085001.

[12] HOANG, G.T., BOURDELLE, C., BEURSKENS, M., *et al.*, "Experimental determination of critical threshold in electron transport on Tore Supra", Phys. Rev. Lett. **87** (2001) 125001

[13] ANGIONI, C., PEETERS, A.G., RYTER, F., *et al.*, "Relationship between density peaking, particle thermodiffusion, Ohmic confinement, and microinstabilities in ASDEX Upgrade L-mode plasmas", Phys. Plasmas **12** (2005) 040701

[14] *NAG Fortran Library Manual*, Mark 19 (The Numerical Algorithms Group Ltd., Oxford, 1999)

[15] DIAMOND, P.H., and HAHM, T.S., "On the dynamics of turbulent transport near marginal stability", Phys. Plasmas **2** (1995) 3640

[16] CARRERAS, B.A., LYNCH, V.E, DIAMOND, P.H., and MEDVEDEV, M., "On the stiffness of the sand pile profile", Phys. Plasmas **5** (1998) 1206